

Geometric Control and Differential Flatness of a Quadrotor UAV with a Cable-Suspended Load

Koushil Sreenath, Taeyoung Lee, Vijay Kumar

Abstract—A quadrotor with a cable-suspended load with eight degrees of freedom and four degrees underactuation is considered and a coordinate-free dynamic model, defined on the configuration space $SE(3) \times S^2$, is obtained by taking variations on manifolds. The quadrotor-load system is established to be a *differentially-flat hybrid system* with the load position and the quadrotor yaw serving as the flat outputs. A nonlinear geometric control design is developed, that enables tracking of outputs defined by (a) quadrotor attitude, (b) load attitude, and (c) position of the load. In each case, the closed-loop system exhibits almost-global properties. Stability proofs for the controller design, as well as simulations of the proposed controller are presented.

I. INTRODUCTION

The introduction of inexpensive micro unmanned aerial vehicles (UAV), such as quadrotors, in recent years has led to a wide range of applications in society. In the area of aerial manipulation, quadrotors have been used for transportation of external loads. By equipping quadrotors with grippers, grasping and transportation of external loads is possible, see [10]. However, carrying an external load through a gripper increases the inertia of the system and results in the quadrotor exhibiting a sluggish attitude response, thereby making it less robust to reject perturbations. An alternative is to suspend loads through a cable, thereby retaining the agility of the aerial vehicle while still achieving the task of transportation of the suspended load.

Cable-suspended systems are underactuated, and several control approaches have been presented in the literature. However, early work is split into controllers that rapidly stabilize load swing [16], [17], and/or trajectory generation schemes that achieve fast motion of the load with minimal swing through preshaping [18], [13], [15]. Control design for suspended load transportation using helicopters and quadrotors has been presented in [1], and [12]. However, the primary focus of this early research has been to minimize the load swing through a combination of trajectory generation and active feedback control.

In this paper, we are particularly interested in the design of controllers for achieving tracking of arbitrarily load

Koushil Sreenath, Mechanical Engineering, Carnegie Mellon University, Pittsburgh, PA 15213, koushils@cmu.edu.

Taeyoung Lee, Mechanical and Aerospace Engineering, George Washington University, Washington, DC 20052, tylee@gwu.edu.

Vijay Kumar, GRASP Lab, University of Pennsylvania, Philadelphia, PA 19104, kumar@seas.upenn.edu.

This research has been supported in part by NSF grants CMMI-1243000 (transferred from 1029551), CMMI-1335008, CNS-1337722, 1113830 and 1138110, ONR grants N00014-07-1-0829 and N00014-08-1-0696, and ARL Grant W911NF-08-2-0004.

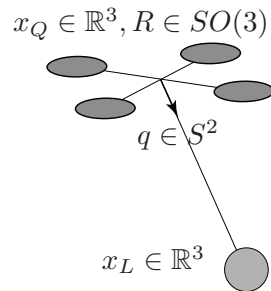


Fig. 1: A quadrotor with a cable suspended load. When the cable is taut, the system evolves on $SE(3) \times S^2$, and has 8 degrees of freedom with 4 degrees of underactuation.

trajectories, while allowing the load to potentially undergo large dynamic swings. Planning trajectories and designing controllers to enable the load to track these trajectories is hard due to the underactuated nature of the problem, and the switching dynamics that arise when the cable is not taut. In our previous paper [14], we developed a controller and presented experimental results for the planar case of the quadrotor with a cable-suspended load, here we present a geometric control design for the full 3D problem.

This paper builds on the earlier geometric control results for position tracking of a quadrotor [6], and develops a coordinate-free dynamic model of the quadrotor with a cable suspended load. This prevents the problem of singularities that are inherent when using local coordinates, and enables designing controllers offering almost-global convergence properties. For the quadrotor with the cable suspended load, the dynamics evolve either on $SE(3) \times S^2$, or $SE(3) \times \mathbb{R}^3$, depending on if the cable is taut or not. We show that the quadrotor with cable-suspended load system is a *differentially-flat hybrid system*. This enables dynamic trajectory generation that also handles the case when the tension in the cable goes to zero. The main result of this paper is the development of a geometric controller design for tracking outputs specified by (a) the quadrotor attitude, (b) the load attitude, and (c) the load position. The controller for tracking the quadrotor attitude and load attitude exhibits almost-global exponential stability, while the load position control exhibits almost-global exponential attractivity.

In a companion paper [8], we extend the control results developed here to the case of multiple quadrotors. In particular, the case of n cooperating quadrotors with a single suspended load is considered, and a controller is developed for asymptotic tracking of the load position.

The paper is organized as follows. Section II develops a coordinate-free dynamical model for the system comprised of

| | |
|-----------------------------------|--------------------------------------------------------------------------------------------|
| $m_Q \in \mathbb{R}$ | Mass of the quadrotor |
| $J_Q \in \mathbb{R}^{3 \times 3}$ | Inertia matrix of the quadrotor with respect to the body-fixed frame |
| $R \in SO(3)$ | Rotation matrix of the quadrotor from body-fixed frame to the inertial frame |
| $\Omega \in \mathbb{R}^3$ | Angular velocity of the quadrotor in the body-fixed frame |
| $x_Q, v_Q \in \mathbb{R}^3$ | Position and velocity vectors of the center of mass of the quadrotor in the inertial frame |
| $f \in \mathbb{R}$ | Magnitude of the thrust for the quadrotor |
| $M \in \mathbb{R}^3$ | Moment vector for the quadrotor in the body-fixed frame |
| $m_L \in \mathbb{R}$ | Mass of the suspended load |
| $q \in S^2 \subset \mathbb{R}^3$ | Unit vector from quadrotor to the load |
| $\omega \in \mathbb{R}^3$ | Angular velocity of the suspended load |
| $x_L, v_L \in \mathbb{R}^3$ | Position and velocity vectors of the suspended load in the inertial frame |
| $l \in \mathbb{R}$ | Length of the suspension cable |
| $T \in \mathbb{R}$ | Tension in the cable. |

TABLE I: Definition of various symbols used in the paper.

a quadrotor with a cable suspended load. Section III demonstrates that the system under consideration is a differentially-flat hybrid system. Section IV presents the main result of the geometric control design. Section V studies the effect of evolution of the quadrotor trajectory that is required to track a given load trajectory at different frequencies. Finally, Section VI presents concluding remarks.

II. DYNAMIC MODEL OF A QUADROTOR WITH CABLE SUSPENDED LOAD

We develop a coordinate-free dynamic model for the quadrotor with a cable suspended load by using rotation matrices for representing the quadrotor attitude and the two-sphere for representing the load attitude. Consider the system depicted by Figure 1, with the various symbols defined in Table I. A hybrid model of this system is developed by first developing the the dynamic models for the cases when the tension in the cable is nonzero, and when the tension is zero.

A. Dynamical Model with Nonzero Cable Tension

The configuration of the system is defined by the location of the load with respect to the inertial frame, the load attitude and the quadrotor attitude. When the cable is taut, the system has eight degrees of freedom with configuration space $Q = SE(3) \times S^2$, and four degree underactuation. The quadrotor and load positions are related by

$$x_Q = x_L - lq, \quad (1)$$

where the various symbols are as defined in Table I. The method of Lagrange is used to develop the equations of motion. The Lagrangian for the system, $\mathcal{L} : TQ \rightarrow \mathbb{R}$, is defined by $\mathcal{L} = \mathcal{T} - \mathcal{U}$, where $\mathcal{T} : TQ \rightarrow \mathbb{R}$ and $\mathcal{U} : Q \rightarrow \mathbb{R}$ are the kinetic and potential energies of the mechanism, respectively, and are defined as,

$$\mathcal{T} = \frac{1}{2}m_Q v_Q \cdot v_Q + \frac{1}{2}m_L v_L \cdot v_L + \frac{1}{2}\langle \hat{\Omega}, \widehat{J_Q \Omega} \rangle, \quad (2)$$

$$\mathcal{U} = m_Q g e_3 \cdot x_Q + m_L g e_3 \cdot x_L, \quad (3)$$

where v_Q is obtained as the derivative of (1), $\langle \cdot, \cdot \rangle : \mathfrak{so}(3) \times \mathfrak{so}(3) \rightarrow \mathbb{R}$ is the inner product on $\mathfrak{so}(3)$, and the *hat map*

$\hat{\cdot} : \mathbb{R}^3 \rightarrow \mathfrak{so}(3)$ is defined such that $\hat{x}y = x \times y, \forall x, y \in \mathbb{R}^3$. Throughout this paper, $\lambda_m(\cdot)$ and $\lambda_M(\cdot)$ denote the minimum and maximum eigenvalue of a matrix respectively.

The dynamics of the system satisfy the Lagrange-d'Alembert principle,

$$\delta \int_0^\tau \mathcal{L} dt + \int_0^\tau \left(\langle W_1, \hat{M} \rangle + W_2 \cdot f R e_3 \right) dt = 0, \quad (4)$$

where f is the thrust magnitude, M is the moment vector, and $W_1 = R^T \delta R$, $W_2 = \delta x_Q = \delta x_L - l \delta q$ are variational vector fields [11], with the infinitesimal variations satisfying [6], [2], [7]

$$\delta q = \xi \times q, \quad \xi \in \mathbb{R}^3 \text{ s.t. } \xi \cdot q = 0$$

$$\delta \dot{q} = \dot{\xi} \times q + \xi \times \dot{q}$$

$$\delta R = R \hat{\eta}, \quad \eta \in \mathbb{R}^3$$

$$\delta \hat{\Omega} = \widehat{\Omega \eta} + \hat{\eta},$$

with δq being a variation on S^2 , and δR a variation on $SO(3)$.

Since (4) is satisfied for all possible variations, the equations of motion for the quadrotor with cable-suspended load are obtained as

$$\dot{x}_L = v_L, \quad (5)$$

$$(m_Q + m_L)(\dot{v}_L + g e_3) = (q \cdot f R e_3 - m_Q l(\dot{q} \cdot \dot{q}))q, \quad (6)$$

$$\dot{q} = \omega \times q, \quad (7)$$

$$m_Q l \dot{\omega} = -q \times f R e_3, \quad (8)$$

$$\dot{R} = R \hat{\Omega}, \quad (9)$$

$$J_Q \dot{\Omega} + \Omega \times J_Q \Omega = M. \quad (10)$$

For developing the hybrid model, the above dynamics can be written in the standard form, $\dot{X}_n = f_n(X_n) + g_n(X_n)u$, where $X_n = \{x_L, q, R, v_L, \omega, \Omega\}$ is the state, and $u = \{f, M\}$ the input of the system receptively.

Remark 1: Note that the quadrotor attitude dynamics, (10), is decoupled from the load position and attitude dynamics, (6) and (8), while the load attitude dynamics is decoupled from the load position dynamics. Also notice that gravity does not influence the load attitude dynamics. Both these observations will motivate the choice of our control structure in Section IV.

Remark 2: The load attitude dynamics (8) can also be written directly in terms of the load attitude, $q \in S^2$, and its derivatives as,

$$m_Q l \ddot{q} + m_Q l(\dot{q} \cdot \dot{q})q = q \times (q \times f R e_3), \quad (11)$$

This equation for the load attitude dynamics will be used for control design.

B. Dynamical Model with Zero Cable Tension

When the tension in the cable goes to zero, the system evolves on $Q_z = SE(3) \times \mathbb{R}^3$, with the quadrotor and load

as separate systems, with the load being in free fall. The dynamical model in this case is,

$$\dot{x}_L = v_L, \quad m_L(\dot{v}_L + ge_3) = 0, \quad (12)$$

$$\dot{x}_Q = v_Q, \quad m_Q(\dot{v}_Q + ge_3) = fRe_3, \quad (13)$$

$$\dot{R} = R\hat{\Omega}, \quad J_Q\dot{\hat{\Omega}} + \hat{\Omega} \times J_Q\hat{\Omega} = M. \quad (14)$$

The above dynamics can also be written in the standard form, $\dot{X}_z = f_z(X_z) + g_z(X_z)u$, where $X_z = \{x_L, x_Q, R, v_L, v_Q, \hat{\Omega}\}$ is the state.

C. Hybrid Model

The quadrotor with a cable suspended load is a hybrid system since the dynamics switch when the tension in the cable drops to zero or when the slack cable becomes taut when the tension gets reestablished. The hybrid model can be written as,

$$\Sigma_n : \begin{cases} \dot{X}_n = f_n(X_n) + g_n(X_n)u, & X_n \notin S_z \\ X_n^+ = \Delta_{n \rightarrow z}(X_n^-), & X_n \in S_z \end{cases}$$

$$\Sigma_z : \begin{cases} \dot{X}_z = f_z(X_z) + g_z(X_z)u, & X_z \notin S_n \\ X_n^+ = \Delta_{z \rightarrow n}(X_z^-), & X_z \in S_n, \end{cases}$$

where the guards are defined as $S_z = \{X_n \mid T \equiv 0\}$, $S_n = \{X_z \mid \|x_Q - x_L\| \equiv l, \frac{d}{dt}\|x_Q - x_L\| > 0\}$, and the tension $T := \|m_L(\ddot{x}_L + ge_3)\|$. The transition map $\Delta_{n \rightarrow z}$ is an identity map, while $\Delta_{z \rightarrow n}$ is modeled as an inelastic collision of two objects, that ensures $\dot{x}_Q^+ - \dot{x}_L^+ = 0$.

Next, we demonstrate that the quadrotor with a cable suspended load is differentially flat with the load position and the quadrotor yaw angle being the flat outputs. Moreover we will also show that this is a differentially flat hybrid system.

III. DIFFERENTIAL FLATNESS

A system is differentially-flat, if there exists a set of outputs such that the system states and the inputs can be expressed in terms of the flat output and a finite number of its derivatives [4]. Here we will briefly present differential flatness for the quadrotor with a cable suspended load, as developed in our earlier work for the planar system [14].

Definition 1: A *Differentially-Flat Hybrid System* is a hybrid system where each subsystem is differentially-flat, with the guards being functions fo the flat outputs and their derivatives, and moreover there are sufficiently smooth transition maps from the flat output space of one subsystem to the flat output space of the subsequent subsystem.

Remark 3: A differentially-flat hybrid system does not imply that all the states and inputs of the system can be obtained by differentiating a set of smooth flat outputs. The system is hybrid after all, and we expect discrete jumps in the states and inputs. Instead, we mean that each subsystem is differentially flat, and that the flat outputs of a subsequent subsystem arise as smooth functions of the flat outputs of the current subsystem mapped through the transition map between the two subsystems.

Lemma 1: The system comprising of a quadrotor with a cable suspended load is a differentially flat hybrid system.

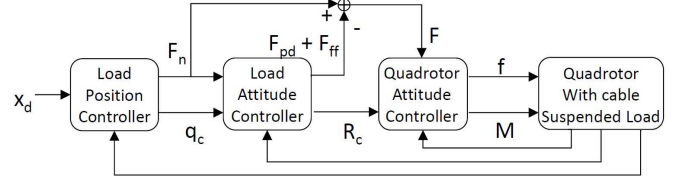


Fig. 2: Controller structure for tracking load position.

Proof: $\mathcal{Y} = (x_L, \psi)$ is a set of flat outputs for the quadrotor with a cable syspended load [14, Lemma 1]. This implies that the event when $X \in S_z$ is known, since the tension is a function of the above flat outputs. Next, for the free quadrotor and load system, the evolution of the quadrotor is known from $\mathcal{Y}_Q = (x_Q, \psi)$ (since \mathcal{Y}_Q is a set of flat outputs for the quadrotor [9]), and the evolution of the load is known from its post-transition state since it undergoes ballistic motion. From this, the transition event $X_z \in S$ is also known, thereby making this a differentially-flat hybrid system. ■

In Section V, we use the flatness property of the system under consideration to see how the quadrotor trajectory evolves when the frequency of the designed load trajectory is modified.

IV. CONTROL DESIGN

Having derived the dynamics of a general 3-dimensional quadrotor with a cable suspended load system and shown that the load position forms a set of differentially-flat outputs for the system, we will develop a controller that can be used for tracking one of the following quantities (a) quadrotor attitude, (b) load attitude, or (c) load position. Figure 2 illustrates the inner-outer loop controller structure for the load position tracking.

Before proceeding to describe the controller, we will first define configuration error functions on the Manifolds $SO(3)$ and S^2 , see [2], as follows. The configuration error on $SO(3)$ is given as, $\Psi_R = \frac{1}{2} \text{Tr}(I - R_d^T R)$, while e_R, e_Ω are error functions on $TSO(3)$, and are given by,

$$e_R = \frac{1}{2}(R_d^T R - R^T R_d)^\vee, \quad (15)$$

$$e_\Omega = \Omega - R^T R_d \Omega_d, \quad (16)$$

where R_d and Ω_d are the desired orientation and angular velocity of the quadrotor respectively. Similarly, the configuration error on S^2 is given as, $\Psi_q = 1 - q_d^T q$, while $e_q, e_{\dot{q}}$ are error functions on TS^2 , and are given by,

$$e_q = \hat{q}^2 q_d, \quad (17)$$

$$e_{\dot{q}} = \dot{q} - (q_d \times \dot{q}_d) \times q, \quad (18)$$

where q_d is the desired load orientation. For use later, we also define the tracking errors for position and velocity respectively as,

$$e_x = x - x_d, \quad (19)$$

$$e_v = v - v_d, \quad (20)$$

where $x_d(t) \in \mathbb{R}^3$ is some smooth desired load position, and $v_d = \dot{x}_d$.

Proposition 1: [6, Prop. 1] (*Almost Global Exponential Stability of Quadrotor Attitude Controlled Flight Mode*) Consider the quadrotor dynamical model in (10), and consider the moment defined as

$$M = -\frac{1}{\epsilon^2}k_R e_R - \frac{1}{\epsilon}k_\Omega e_\Omega + \Omega \times J_Q \Omega - J_Q(\hat{\Omega} R^T R_d \Omega_d - R^T R_d \hat{\Omega}_d), \quad (21)$$

for any positive constants k_R , k_Ω , and $0 < \epsilon < 1$. Further, suppose the initial conditions satisfy

$$\Psi_R(R(0), R_d(0)) < 2 \quad (22)$$

$$\|e_\Omega(0)\|^2 < \frac{2}{\lambda_M(J_Q)} \frac{k_R}{\epsilon^2} (2 - \Psi_R(R(0), R_d(0))). \quad (23)$$

Then, the zero equilibrium of the closed loop tracking error $(e_R, e_\Omega) = (0, 0)$ is exponentially stable. Furthermore, there exist constants $\alpha_R, \beta_R > 0$ such that,

$$\Psi_R(R(t), R_d(t)) \leq \min \{2, \alpha_R e^{-\beta_R t}\}. \quad (24)$$

The domain of attraction is characterized by (22), (23). Moreover, the region of statespace $TSO(3)$ that does not converge to the equilibrium is of measure zero, resulting in almost global exponential stability.

Proof: The controller (21) is a geometric version of PD control along with a feedforward term. The proof follows directly from [6, Prop. 1] after defining $k_R^\epsilon = \frac{1}{\epsilon^2}k_R$, $k_\Omega^\epsilon = \frac{1}{\epsilon}k_\Omega$. The ϵ parameter is introduced to enable rapid exponential convergence, which will be employed for a singular perturbation argument in the following Propositions. ■

Proposition 2: (*Almost Global Exponential Stability of Load Attitude Controlled Flight Mode*) Consider the load attitude dynamics in (8), and consider the computed quadrotor attitude defined as

$$R_c := [b_{1_c}; b_{3_c} \times b_{1_c}; b_{3_c}], \quad \hat{\Omega}_c = R_c^T \dot{R}_c \quad (25)$$

where $b_{3_c} \in S^2$ is defined by

$$b_{3_c} = \frac{F}{\|F\|}, \quad (26)$$

where,

$$F = F_n - F_{pd} - F_{ff}, \quad (27)$$

where F_n , F_{pd} and F_{ff} are as defined below

$$F_n = -(q_d \cdot q)q \quad (28)$$

$$F_{pd} = -k_q e_q - k_\omega e_{\dot{q}} \quad (29)$$

$$F_{ff} = m_Q l \langle q, q_d \times \dot{q}_d \rangle (q \times \dot{q}) + m_Q l (q_d \times \ddot{q}_d) \times q. \quad (30)$$

We also choose $b_{1_d} \in S^2$, not parallel to b_{3_c} and define the unit vector b_{1_c} as

$$b_{1_c} = -\frac{1}{\|b_{3_c} \times b_{1_d}\|} (b_{3_c} \times (b_{3_c} \times b_{1_d})). \quad (31)$$

Now, consider the quadrotor thrust f is defined by

$$f = F \cdot R e_3, \quad (32)$$

with the quadrotor moment defined by (21) with the computed values, R_c, Ω_c used instead of the desired ones. Further, suppose the initial conditions satisfy

$$\Psi_q(q(0), q_d(0)) < 2, \quad (33)$$

$$\|e_{\dot{q}}(0)\|^2 < \frac{2}{m_Q l} k_q (2 - \Psi_q(q(0), q_d(0))). \quad (34)$$

Then, there exists $\bar{\epsilon}_q$, such that for all $0 < \epsilon < \bar{\epsilon}_q$, the zero equilibrium of the closed loop tracking error $(e_q, e_{\dot{q}}, e_R, e_\Omega) = (0, 0, 0, 0)$ is exponentially stable. Furthermore, there exist constants $\alpha_q, \beta_q > 0$ such that,

$$\Psi_q(q(t), q_d(t)) \leq \min \{2, \alpha_q e^{-\beta_q t}\}. \quad (35)$$

The domain of attraction is characterized by (22), (23), (33), (34). Moreover, the region of statespace $TS^2 \times TSO(3)$ that does not converge to the equilibrium is of measure zero, resulting in almost global exponential stability.

Proof: See Appendix I-A. ■

We have exponential stability for all initial load attitudes such that (33) is satisfied. This basically means the initial load attitude error should be less than 180° . Since the load attitudes that lie outside the region of attraction are of the form $q_d(0) = -q(0)$, which is a low-dimensional manifold in $TS^2 \times TSO(3)$, and is of measure zero. Thus the controller achieves almost global exponential convergence for load attitude.

The inclusion of a normal component F_n in (27) ensures that b_{3_c} is always well defined. Moreover, since F_n is along q , it has no effect on the load attitude dynamics.

Also notice that in order to obtain exponential stability of the load attitude, both the quadrotor moment and the quadrotor thrust were specified. This raises the question of if and how load position can be tracked, especially since we have no other inputs. To answer this, notice from (8), that any force, $f R e_3$ that is along q does not influence the load attitude dynamics. Also notice that from (6), any force tangential to q does not influence the load position dynamics. This fact will be used in the following.

Proposition 3: (*Exponential Stability of Load Position Controlled Flight Mode*) Consider the load position dynamics in (6), and consider the computed load attitude defined as

$$q_c = -\frac{A}{\|A\|}, \quad (36)$$

where

$$A = -k_x e_x - k_v e_v + (m_Q + m_L)(\ddot{x}_L^d + g e_3) + m_Q l (\dot{q} \cdot \dot{q})q, \quad (37)$$

with $e_x = x_L - x_L^d$, and $e_v = v_L - v_L^d$ being the error in the load position and velocity respectively. We assume $\|A\| \neq 0$, and the commanded acceleration is uniformly bounded such that

$$\|(m_Q + m_L)(\ddot{x}_L^d + g e_3) + m_Q l (\dot{q} \cdot \dot{q})q\| < B.$$

Furthermore, define F_n in (27) as

$$F_n = (A \cdot q)q. \quad (38)$$

Let the computed quadrotor attitude be defined by (25), (26), with the quadrotor thrust and moment defined by (32) and (21), with the desired quadrotor and load attitude replaced by their computed values, R_c , and q_c respectively. Further, suppose the initial conditions satisfy

$$\Psi_q(q(0), q_c(0)) < \psi_1 < 1, \quad (39)$$

$$\|e_x(0)\| < e_{x_{max}}, \quad (40)$$

for a fixed constant $e_{x_{max}}$. Define $W_x, W_{xq} \in \mathbb{R}^{2 \times 2}$ as,

$$W_x = \begin{bmatrix} \frac{c_1 k_x}{m_Q + m_L} (1 - \alpha) & -\frac{c_1 k_v}{2(m_Q + m_L)} (1 + \alpha) \\ -\frac{c_1 k_v}{2(m_Q + m_L)} (1 + \alpha) & k_v (1 - \alpha) - c_1 \end{bmatrix}, \quad (41)$$

$$W_{xq} = \begin{bmatrix} \frac{c_1}{m_Q + m_L} & 0 \\ K_x e_{x_{max}} + B & 0 \end{bmatrix}, \quad (42)$$

where $\alpha := \sqrt{\psi_1(2 - \psi_1)}$, and c_1, k_x, k_v are positive constants such that,

$$c_1 < \min \left\{ k_v (1 - \alpha), \sqrt{k_x (m_Q + m_L)}, \frac{4(m_Q + m_L) k_x k_v (1 - \alpha)}{k_v^2 (1 - \alpha)^2 + 4(m_Q + m_L) k_x} \right\} \quad (43)$$

$$\lambda_m(W_q) > \frac{\|W_{xq}\|^2}{4\lambda_m(W_x)}. \quad (44)$$

Then, there exists $\bar{\epsilon}_x$, such that for all $0 < \epsilon < \bar{\epsilon}_x$, the zero equilibrium of the closed loop tracking error $(e_x, e_v, e_q, e_{\dot{q}}, e_R, e_\Omega) = (0, 0, 0, 0, 0, 0)$ is exponentially stable. The domain of attraction is characterized by (22), (23), with the desired values replaced by the computed values, (39), and

$$\|e_{\dot{q}}(0)\|^2 < \frac{2}{m_Q l} k_q (\psi_1 - \Psi_q(q(0), q_c(0))). \quad (45)$$

Proof: See Appendix I-B. ■

Remark 4: If the load is connected to the quadrotor through a rigid link, then by changing the sign in (36), we obtain a controller for tracking the position of the tip of a spherical inverted pendulum on a quadrotor. Further results on this are presented in the companion paper [8].

Proposition 4: (Almost Global Exponential Attractiveness of Load Position Controlled Flight Mode) Consider the quadrotor thrust f and moment M defined in expressions (32), (21). Suppose the initial conditions satisfy (22), (23), (33), (34). Then, zero equilibrium of the closed loop tracking error $(e_x, e_v, e_q, e_{\dot{q}}, e_R, e_\Omega) = (0, 0, 0, 0, 0, 0)$ is exponentially attractive.

Proof: See Appendix I-C. ■

Remark 5: Note that the controller presented here, in combination with the controller in [6] offering almost-global exponential attractivity of the quadrotor position controlled flight mode, ensures a control design for the full hybrid system.

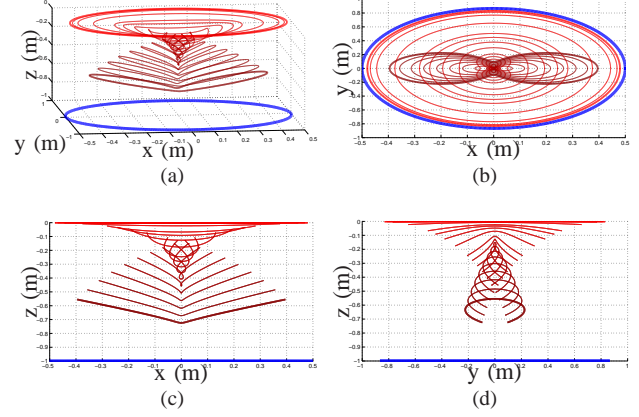


Fig. 3: Evolution of the trajectories of a quadrotor (red) required to track the load trajectory (blue) as the time period of load trajectory is varied from 10 seconds to 1 second. The figures show the plots in different views. Note that the trajectories become far more aggressive as the desired load trajectory time period goes from 10 seconds to 1 second.

V. RESULTS

A. Trajectory Generation using Differential Flatness

Since the quadrotor and load system is differentially flat, we can plan and study trajectories directly in the flat space. We could do this through parametrizing the flat outputs as functions of time with a suitable basis and solving an optimization problem to obtain the coefficients of the basis, as done in [9] for a quadrotor. However, our aim is to study how the quadrotor trajectory, required to track a particular load trajectory, evolves as the frequency of the load trajectory varies. In particular, we chose the flat outputs as follows,

$$x_L(t) = \begin{bmatrix} A_x \sin\left(\frac{2\pi t}{T_0}\right) \\ A_y \cos\left(\frac{2\pi t}{T_0}\right) \\ A_z \end{bmatrix} \quad (46)$$

$$\psi(t) \equiv 0, \quad (47)$$

where, T_0 is the time period of oscillation of the load. Using the differential-flatness property, we can analytically obtain the quadrotor trajectories for the corresponding flat outputs. Moreover, by varying the time period, we can study the evolution of the quadrotor trajectories. Figure 3 illustrates the quadrotor trajectories for multiple time periods, from 1 to 10 seconds, for following the load trajectory specified in (46), with $A_x < A_y$. The quadrotor trajectories dynamically evolve and become far more aggressive for smaller time periods. Note that all the different quadrotor trajectories result in the same load trajectory, albeit at different frequency of oscillation of the load.

B. Load Position Controlled Flight Mode

Next, we present a simulation with the initial condition specifying large errors in the quadrotor attitude, the load attitude and the load position. Specifically, the quadrotor is starts off flipped about the y-axis at 178° , the load attitude is specified as 178° , and there is a large initial load position error. A desired time-varying load position trajectory is

VI. CONCLUSION

We have presented a coordinate-free development of the dynamics of a quadrotor with a cable suspended load, and have shown that this system is a differentially-flat hybrid system. The flatness property has been utilized to design nominal trajectories. A nonlinear geometric control design is presented, that enables tracking of either the quadrotor attitude, the load attitude or the position of the load. Almost global exponential stability for the load attitude tracking, and almost global exponential attractivity of the load position tracking is demonstrated.

APPENDIX I

A. Proof of Proposition 2

We begin by representing the load attitude dynamics (8) as

$$\begin{bmatrix} \dot{q} \\ \dot{\omega} \end{bmatrix} =: f(q, \omega, R) = \begin{bmatrix} \omega \times q \\ -\frac{1}{m_Q l} q \times (F \cdot R e_3) R e_3 \end{bmatrix}. \quad (48)$$

Next, From Proposition 1, and [6, Prop. 1], and defining $\bar{e}_R = \frac{1}{\epsilon} e_R$, the closed-loop quadrotor error dynamics can be represented as

$$\epsilon \begin{bmatrix} \dot{\bar{e}}_R \\ \dot{\bar{e}}_\Omega \end{bmatrix} =: g(R, \Omega, \epsilon) = \begin{bmatrix} \frac{1}{2} (R_c^T R \hat{e}_\Omega + \hat{e}_\Omega R^T R_c)^\vee \\ -k_R \bar{e}_R - k_\Omega \bar{e}_\Omega \end{bmatrix}. \quad (49)$$

Setting ϵ to zero, we get,

$$0 = g(R, \Omega, 0) \implies R \equiv R_c. \quad (50)$$

In the limit $\epsilon = 0$, the load attitude dynamics evolves on the manifold given by $R \equiv R_c$. In particular, the *slow model* is

$$\begin{bmatrix} \dot{q} \\ \dot{\omega} \end{bmatrix} = f(q, \omega, R_c) = \begin{bmatrix} \omega \times q \\ -\frac{1}{m_Q l} q \times (F \cdot R_c e_3) R_c e_3 \end{bmatrix}. \quad (51)$$

The rest of the proof will establish exponential stability for the slow model from [2, Lemma 11.23] and then through a singular perturbation argument (Tychonoff Theorem) [5, Thm. 11.2], the trajectories of the full system will be shown to uniformly converge to that of the slow model, establishing exponential convergence for the full model.

From the load attitude dynamics, (11), the input force enters the system through $q \times (q \times F R e_3)$. For the slow model, this can be written as,

$$\begin{aligned} q \times (q \times (F \cdot R_c e_3) R_c e_3) &= q \times (q \times F) \\ &= -k_q e_q - k_d e_\omega + F_f \end{aligned} \quad (52)$$

where we have used the following facts, $\hat{q}^2 F_n = 0$, $\hat{q}^2 e_q = -e_q$, $\hat{q}^2 e_{\hat{q}} = -e_{\hat{q}}$, $\hat{q}^2 F_{ff} = -F_{ff}$, since $e_q, e_{\hat{q}}, F_{ff} \in T_q S^2$ and $q \times F_n = 0$. Further, since the norm of $b_{3c} \in S^2$ in the denominator is bounded away from zero, then for $k_q > 0$, $k_d > 0$, exponential convergence follows from [2, Lemma 11.23]. Then, by the converse Lyapunov Theorems, there exists a Lyapunov function \mathcal{V}_q and positive definite matrices M_q, M_Q, W_q , such that

$$z_q^T M_q z_q \leq \mathcal{V}_q \leq z_q^T M_Q z_q \quad (53)$$

$$\dot{\mathcal{V}}_q \leq -z_q^T W_q z_q, \quad (54)$$

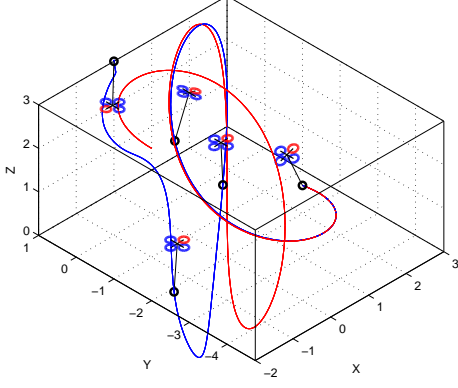


Fig. 4: Snapshots of the quadrotor along the executed motion (blue) as it tracks the desired load position (red). Notice the large initial errors in position, load and quadrotor attitude. The quadrotor and the load start off almost flipped.

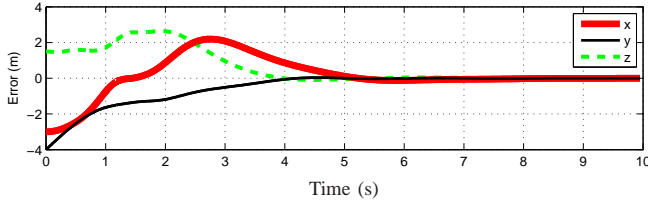


Fig. 5: Load position error tracking. Notice the initial large position errors that are quickly rejected by the controller.

specified and the system is simulated with the controller in Proposition 3. Figure 4 illustrates the trajectory of the load as it converges to the desired load position trajectory, as well as snapshots of the quadrotor at fixed intervals. Figure 5 illustrates the load position error, while Figure 6 illustrates the configuration error metric for the quadrotor and load attitudes respectively. Note that the double peak in Ψ_R and Ψ_q occur due to the controller implementation not computing $\dot{R}_c, \ddot{R}_c, \dot{q}_c, \ddot{q}_c$, but rather using the nominal values from differential-flatness. This results in a simpler controller implementation. The command derivatives can be computed through a command filtering approach [3], or by carrying out the complex task of analytically computing the derivatives, as is done in the companion paper [8]. Nevertheless, the simpler controller implementation is able to reject the large errors in load position, load attitude and quadrotor attitude.

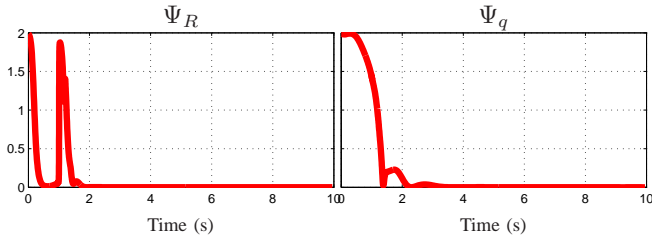


Fig. 6: Configuration error functions for the quadrotor attitude and the load attitude. Controller rejects large attitude errors of 178° in both the quadrotor and load attitudes.

where $z_q = [\|e_q\|, \|e_{\dot{q}}\|]^T$.

Remark 6: Note that this proposition would still hold for other choices of F_n . In particular, it holds for the choice in (38).

Thus, for the slow model, $(e_q, e_{\dot{q}})$ exponentially converges to zero. Now, for the full model, since the slow model satisfies the conditions of [5, Thm. 11.2], there exists $\bar{\epsilon}_q > 0$, such that, for all $0 < \epsilon < \bar{\epsilon}_q$, the trajectories of full model, $(q, \omega, R, \Omega)(t)$ and the trajectories of the slow model, $(q, \omega, R_c, \Omega_c)(t)$ satisfy $(q, \omega, R, \Omega)(t) - (q, \omega, R_c, \Omega_c)(t) = O(\epsilon)$ uniformly. This results in exponential stability of the load attitude dynamics for the full model.

B. Proof of Proposition 3

This proof is motivated by the proof of [6, Prop. 3], and follows it very closely. While [6, Prop. 3] was proving exponential stability of the quadrotor position, here we address a more complex system with additional underactuation and demonstrate exponential stability of the complete system through a singular perturbation argument.

We will consider the slow model and carry out the subsequent analysis in the domain

$$D = \{(e_x, e_v, q, e_{\dot{q}}) \in \mathbb{R}^3 \times \mathbb{R}^3 \times L_1 \times \mathbb{R}^3 \mid \|e_x\| < e_{x_{max}}\}, \quad (55)$$

where, by (39), the load attitude is restricted to be in the sublevel set $L_1 = \{q \in S^2 \mid \Psi_q(q, q_c) < 1\}$.

Translational Error Dynamics for Slow Model The translational error dynamics of the complete system is given by

$$\begin{aligned} \dot{e}_x &= e_v & (56) \\ (m_Q + m_L)\dot{e}_v &= -(m_Q + m_L)(ge_3 + \ddot{x}_L^d) \\ &\quad - m_Q l(\dot{q} \cdot \dot{q})q + (q \cdot f)Re_3. \end{aligned} \quad (57)$$

Considering the slow model, where in the limit $\epsilon = 0$, the load position and attitude dynamics evolve on the manifold given by $R \equiv R_c$, we have from (26)

$$Re_3 \equiv R_c e_3 = b_{3_c} = \frac{F}{\|F\|}.$$

Also from (32), we have

$$f = F \cdot Re_3 \equiv F \cdot R_c e_3 = f \cdot b_{3_c} = F \cdot \frac{F}{\|F\|} = \|F\|.$$

Then,

$$fRe_3 \equiv fR_c e_3 = fb_{3_c} = \|F\| \frac{F}{\|F\|} = F.$$

Finally,

$$\begin{aligned} (q \cdot f)Re_3 q &= (q \cdot F)q \\ &= (q \cdot (F_n + F_{pd} - F_{ff}))q \\ &= (A \cdot q)q \\ &=: f_q q. \end{aligned} \quad (58)$$

Furthermore, by (39), the quantity $\frac{1}{q_c^T q}$ is well defined. Then, to rewrite the error dynamics of e_v in terms of the load

attitude error e_q , we add and subtract $\frac{f_q}{q_c^T q}$ to the right hand side of (57) obtaining

$$\begin{aligned} (m_Q + m_L)\dot{e}_v &= -(m_Q + m_L)(ge_3 + \ddot{x}_L^d) - m_Q l(\dot{q} \cdot \dot{q})q \\ &\quad + \frac{f_q}{q_c^T q} q_c + X, \end{aligned} \quad (59)$$

where $X \in \mathbb{R}^3$ is defined as

$$X = \frac{f_q}{q_c^T q} ((q_c \cdot q)q - q_c). \quad (60)$$

From the definition of $f_q = A \cdot q$, and from (36), we have

$$f_q = -\|A\|q_c \cdot q. \quad (61)$$

Therefore, the third term on the right hand side of (59) can be written as

$$\frac{f_q}{q_c^T q} q_c = \frac{(-\|A\|q_c \cdot q)}{q_c \cdot q} \cdot -\frac{A}{\|A\|} = A.$$

Substituting this into (59) and using A from (37), the translational error dynamics of e_v can be written as

$$(m_Q + m_L)\dot{e}_v = -k_x e_x - k_v e_v + X. \quad (62)$$

Lyapunov Candidate for Translation Dynamics Consider the Lyapunov candidate \mathcal{V}_x ,

$$\mathcal{V}_x = \frac{1}{2}k_x \|e_x\|^2 + \frac{1}{2}(m_Q + m_L)\|e_v\|^2 + c_1 e_x \cdot e_v, \quad (63)$$

where c_1 is a positive constant. The derivative of \mathcal{V}_x along the solution of (62) is given by

$$\begin{aligned} \dot{\mathcal{V}}_x &= k_x e_x \cdot e_v + e_v \cdot (-k_x e_x - k_v e_v + X) + c_1 e_v \cdot e_v \\ &\quad + \frac{c_1}{m_Q + m_L} e_x \cdot (-k_x e_x - k_v e_v + X) \\ &= -(k_v - c_1)\|e_v\|^2 - \frac{c_1 k_x}{m_Q + m_L} \|e_x\|^2 \\ &\quad - \frac{c_1 k_v}{m_Q + m_L} e_x \cdot e_v + X \cdot \left\{ \frac{c_1}{m_Q + m_L} e_x + e_v \right\}. \end{aligned}$$

Next, we find a bound on X using (60) as follows. From (61), we have,

$$\begin{aligned} \|X\| &\leq \|A\| \|(q_c \cdot q)q - q_c\| \\ &\leq (k_x \|e_x\| + k_v \|e_v\| + B)\|e_q\| \\ &\leq (k_x \|e_x\| + k_v \|e_v\| + B)\alpha, \end{aligned} \quad (64)$$

where we have used (37) for the definition of A , recognized from (17), $e_q = q \times (q \times q_c) = (q_c \cdot q)q - q_c$, and that $\|e_q\|$ represents the sine of the angle between q and q_c , given by $\|e_q\| = \sqrt{\Psi_q(2 - \Psi_q)}$. Thus α is defined as

$\alpha = \sqrt{\psi_1(2 - \psi_1)} < 1$. Substituting this into (64), we have,

$$\begin{aligned} \dot{\mathcal{V}}_x &\leq -(k_v - c_1)\|e_v\|^2 - \frac{c_1 k_x}{m_Q + m_L}\|e_x\|^2 \\ &\quad - \frac{c_1 k_v}{m_Q + m_L} e_x \cdot e_v + (k_x\|e_x\| + k_v\|e_v\| + B)\|e_q\| \\ &\quad \left\{ \frac{c_1}{m_Q + m_L}\|e_x\| + \|e_v\| \right\} \\ &\leq -(k_v(1 - \alpha) - c_1)\|e_v\|^2 - \frac{c_1 k_x}{m_Q + m_L}(1 - \alpha)\|e_x\|^2 \\ &\quad + \frac{c_1 k_v}{m_Q + m_L}(1 + \alpha)\|e_x\|\|e_v\| \\ &\quad + \|e_q\| \left\{ k_x\|e_x\|\|e_v\| + \frac{c_1}{m_Q + m_L}\|e_x\| + B\|e_v\| \right\}. \end{aligned} \quad (65)$$

In the above expression, there is a third-order term, $k_x\|e_q\|\|e_x\|\|e_v\|$. Since we restrict our analysis to the domain D defined in (55), an upper bound for this term is $k_x e_{x_{max}}\|e_q\|\|e_v\|$.

Lyapunov Candidate for the Slow Model Let $\mathcal{V} = \mathcal{V}_x + \mathcal{V}_q$ be the Lyapunov candidate for the slow model. Then, from (53), (54), (63), (65), we have,

$$z_x^T M_x z_x + z_q^T M_q z_q \leq \mathcal{V} \leq z_x^T M_X z_x + z_q^T M_Q z_q \quad (66)$$

$$\dot{\mathcal{V}} \leq -z_x^T W_x z_x + z_x^T W_{xq} z_q - z_q^T W_q z_q, \quad (67)$$

where $z_x = [\|e_x\|, \|e_v\|]^T$, and the matrices W_x , W_{xq} are as in (41), (42), while M_x , M_X are defined as

$$M_x = \frac{1}{2} \begin{bmatrix} k_x & -c_1 \\ -c_1 & m_Q + m_L \end{bmatrix}, \quad (68)$$

$$M_X = \frac{1}{2} \begin{bmatrix} k_x & c_1 \\ c_1 & m_Q + m_L \end{bmatrix}. \quad (69)$$

Exponential Stability From Proposition 2, the matrices M_q , M_Q , W_q are positive definite, while the conditions of Proposition 3, (43), ensure positive definiteness of M_x , M_X . Then the candidate Lyapunov function \mathcal{V} is positive-definite, and

$$\dot{\mathcal{V}} \leq -\lambda_m(W_x)\|z_x\|^2 + \|W_{xq}\|_2\|z_x\|\|z_q\| - \lambda_m(W_q)\|z_q\|^2.$$

The conditions of Proposition 3, (43), (44) ensures positive-definiteness of W_x , and negative-definiteness of $\dot{\mathcal{V}}$. Thus the zero equilibrium of the load position tracking errors of the slow model is exponentially stable, i.e., $(e_x, e_v, e_q, \dot{e}_q)$ exponentially converges to zero while the dynamics evolve on the slow manifold given by $R \equiv R_c$.

Now we employ the singular perturbation argument once again. We have, for the full model, since the slow model satisfies the conditions of [5, Thm. 11.2], there exists $\bar{\epsilon}_x > 0$, such that, for all $0 < \epsilon < \bar{\epsilon}_x$, the trajectories of full model, $(x_L, v_L, q, \omega, R, \Omega)(t)$ and the trajectories of the slow model, $(x_L, v_L, q, \omega, R_c, \Omega_c)(t)$ satisfy $(x_L, v_L, q, \omega, R, \Omega)(t) - (x_L, v_L, q, \omega, R_c, \Omega_c)(t) = O(\epsilon)$ uniformly. This results in exponential stability of the load position dynamics for the full model.

C. Proof of Proposition 4

Once again we consider the slow model, whose dynamics evolve on the slow manifold given by $R \equiv R_c$. The initial condition, (33), is outside the region of attraction specified in Proposition 3, (39), and thus exponential convergence of the load position error can not be guaranteed. However, since the initial load attitude satisfies the conditions of Proposition 2, the load attitude tracking error, z_q is guaranteed to exponentially decrease and enter the region of attraction of Proposition 3 in finite time, say t^* . If we can show that the load position error z_x is bounded in this time, $t \in [0, t^*]$, then exponential attractivity ensures for the slow model.

We can still use a singular perturbation argument during $t \in [0, t^*]$ to ensure $(x_L, v_L, q, \omega, R, \Omega)(t) - (x_L, v_L, q, \omega, R_c, \Omega_c)(t) = O(\epsilon)$ uniformly. This results in bounded z_x for the full model too during $t \in [0, t^*]$. Then, we can conclude exponential attractivity for the full model.

Thus, we only need to show that z_x is bounded for $t \in [0, t^*]$ for the slow model. This can easily be shown by following the proof of [6, Prop. 4] with minor changes.

REFERENCES

- [1] M. Bernard and K. Kondak, "Generic slung load transportation system using small size helicopters," in *IEEE International Conference on Robotics and Automation*, Kobe, Japan, May 2009, pp. 3258–3264.
- [2] F. Bullo and A. D. Lewis, *Geometric Control of Mechanical Systems*. New York-Heidelberg-Berlin: Springer-Verlag, 2004.
- [3] J. A. Farrell, M. Polycarpou, M. Sharma, and W. Dong, "Command filtered backstepping," in *American Control Conference*, Seattle, WA, June 2008, pp. 1923–1928.
- [4] M. Fliess, J. Lévine, P. Martin, and P. Rouchon, "Flatness and defect of non-linear systems: introductory theory and examples," *International journal of control*, vol. 61, pp. 1327–1361, 1995.
- [5] H. K. Khalil, *Nonlinear Control*. New Jersey: Prentice Hall, 2002.
- [6] T. Lee, M. Leok, and N. H. McClamroch, "Geometric Tracking Control of a Quadrotor UAV on SE(3)," in *IEEE Conference on Decision and Control*, Atlanta, GA, 2010, pp. 5420–5425.
- [7] —, "Discrete Control Systems," *Mathematics Complexity and Dynamical Systems*, pp. 143–159, 2011.
- [8] T. Lee, K. Sreenath, and V. Kumar, "Geometric control of cooperating multiple quadrotor uavs with a suspended load," in *IEEE Conference on Decision and Control*, to appear, 2013.
- [9] D. Mellinger and V. Kumar, "Minimum snap trajectory generation and control for quadrotors," in *IEEE International Conference on Robotics and Automation*, Shanghai, China, May 2011, pp. 2520–2525.
- [10] D. Mellinger, Q. Lindsey, M. Shomin, and V. Kumar, "Design, modeling, estimation and control for aerial grasping and manipulation," in *IEEE/RSJ International Conference on Intelligent Robots and Systems*, Sep. 2011, pp. 2668–2673.
- [11] J. Milnor, *Morse Theory*. Princeton: Princeton University Press, 1963.
- [12] I. Palunko, R. Fierro, and P. Cruz, "Trajectory generation for swing-free maneuvers of a quadrotor with suspended payload: A dynamic programming approach," in *IEEE International Conference on Robotics and Automation*, St. Paul, MN, May 2012, pp. 2691–2697.
- [13] J. Schultz and T. Murphey, "Trajectory generation for underactuated control of a suspended mass," in *IEEE International Conference on Robotics and Automation*, St. Paul, MN, May 2012, pp. 123–129.
- [14] K. Sreenath, N. Michael, and V. Kumar, "Trajectory generation and control of a quadrotor with a cable-suspended load - a differentially-flat hybrid system," in *IEEE International Conference on Robotics and Automation*, Karlsruhe, Germany, May 2013, pp. 4873–4880.
- [15] G. Starr, J. Wood, and R. Lumia, "Rapid Transport of Suspended Payloads," in *International Conference on Robotics and Automation*, April 2005, pp. 1394–1399.
- [16] N. Yanai, M. Yamamoto, and A. Mohri, "Feedback Control for Wire-Suspended Mechanism with Exact Linearization," in *International Conference on Intelligent Robots and Systems*, October, 2002, pp. 2213–2218.

- [17] J. Yu, F. L. Lewis, and T. Huang, "Nonlinear Feedback Control of a Gantry Crane," in *American Control Conference*, Seattle, WA, June 1995, pp. 4310–4315.
- [18] D. Zamoski, G. Starr, J. Wood, and R. Lumia, "Rapid Swing-Free Transport of Nonlinear Payloads Using Dynamic Programming," *Journal of Dynamic Systems, Measurement, and Control*, vol. 130, no. 4, p. 041001, 2008.